

LOCAL AND GLOBAL PERSPECTIVES IN FLUID DYNAMICS

H. Keith Moffatt

Isaac Newton Institute for Mathematical Sciences

University of Cambridge, United Kingdom

hkm2@newton.cam.ac.uk

1. INTRODUCTION

It is a great honor to present this Closing Lecture at what has been an outstanding Congress, ICTAM 2000. These Congresses have a proud tradition, going back to Delft 1924, when Prandtl, von Kármán, G. I. Taylor and Burgers initiated the series and laid the ground rules. Since then, every four years, with a brief interlude during World War II, the world mechanics community has gathered together to share its knowledge and to grapple with new emerging problems. This is truly a *global* enterprise, and we can all take pride and pleasure in our involvement in it. The first ICTAM that I was privileged to attend was the tenth in the series, held at Stresa in 1960. And here we are now at the 20th ICTAM and actually the 10th that I have been personally involved in.

The global participation at these Congresses is achieved in each case only through an effective *local* organization. Each Congress, whether at Stresa or Stanford, Lyngby or Haifa, Moscow or Toronto, has had its own distinctive local flavor that remains in the heart of each participant long after the details of individual lectures have faded from the memory. Chicago will be no different in this respect, and I would like to record my personal thanks to Hassan Aref and his great team on the Local Organizing Committee here, who have succeeded in making this 20th and millennial Congress so uniquely memorable.

Locality and globality: the two complementary perspectives whose interplay is essential to the successful running of a World Congress. It is a different kind of locality and globality that I propose to discuss in this lecture; but certain parallels may emerge, and I shall return to the Congress scenario in my closing remarks.

In fluid dynamics, the concept of locality emerges most clearly through what we describe as local similarity solutions of the governing Navier–Stokes equations, and I shall give some examples of these. Although such solutions are generally accurate only within a small sub-region of a fluid domain, nevertheless an understanding of them can be of crucial importance for two reasons: first, they provide a check on the accuracy of numerical solutions computed throughout the fluid domain; and second, they can act as organizing centers for the whole flow field; and knowledge of their structure can provide important clues concerning global features of the flows.

But what are these global features? They are those features that are essentially topological in character, structural properties that are ‘robust’, i.e. insensitive to small perturbations. Again, an understanding of such topological features provides a guide for computation and a possible check on computational accuracy. By way of simple example, consider an incompressible two-dimensional flow on the surface of a sphere. At any instant there are a number of stagnation points, which are of either elliptic or hyperbolic type. Topological considerations tell us that if these stagnation points are ‘non-degenerate’ and if N is the number of elliptic points and M the number of hyperbolic points then $N - M = 2$. A numerical search for stagnation points for a given complex flow can be conducted, and their classification as elliptic or hyperbolic can be achieved, at least in principle. If this process leads to values of N and M with $M < N - 2$, then we know that we must have missed some hyperbolic points. As a first priority, we should always seek to ensure that computed flow properties are compatible with such fundamental topological constraints.

2. LOCAL SIMILARITY SOLUTIONS

I want to focus first on a fascinating problem in which I have been intermittently involved since 1963—this is the problem of flow near a sharp corner. Our Chairman has made a vital distinction (Barenblatt 1979) between two types of similarity solution, which both crop up in this context: similarity solutions of the first kind for which dimensional arguments play a key role; and of the second kind for which a key parameter has to be determined through solution of an eigenvalue problem. The two prototype situations are sketched in Figs. 1(a) and 1(b). The first shows G. I. Taylor’s (1960) ‘paint-scraper’ configuration in which one plane boundary is scraped relative to the other with constant velocity U . Sufficiently near the intersection, the flow is a Stokes flow and the streamfunction $\psi(r, \theta)$ is determined on dimensional grounds in the form

$\psi = Urf(\theta)$, where

$$f(\theta) = \frac{(\alpha^2 - k\theta) \sin \theta - \theta \sin^2 \alpha \cos \theta}{\alpha^2 - \sin^2 \alpha}, \quad k = \frac{1}{2}(2\alpha - \sin 2\alpha). \quad (1)$$

This is evidently, in Barenblatt's terminology, a similarity solution of the first kind.

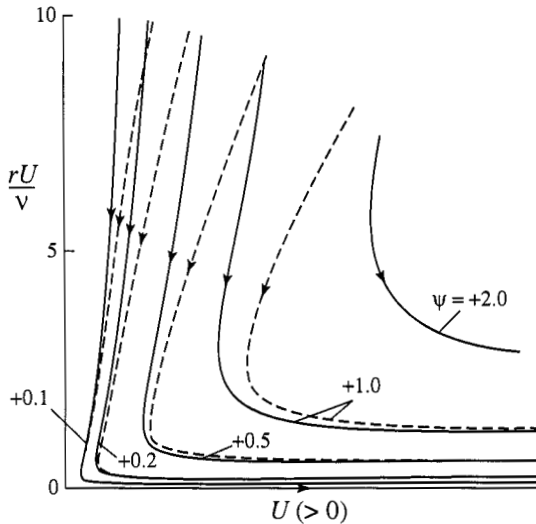


Figure 1(a) Solid curves are the streamlines for the Taylor similarity solution (1); dashed curves show the first-order inertial correction obtained by Hancock, Moffatt, and Lewis (1981).

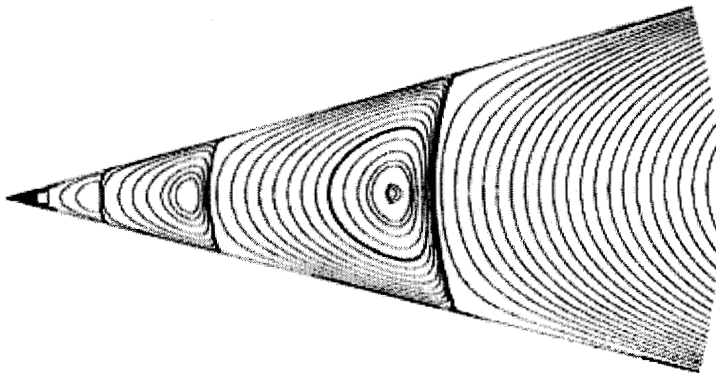


Figure 1(b) Corner eddies described by a similarity solution of the second kind, $\psi \sim r^\lambda f(\theta)$ with λ complex. [Courtesy C. P. Hills]

In Fig. 1(b) by contrast, both boundaries are at rest and fixed at angle α , and a two-dimensional flow is driven by some agency (e.g. a rotating cylinder) far from the corner. In the Stokes approximation, the streamfunction sufficiently near the corner satisfies the biharmonic equation

$$\nabla^4 \psi = 0, \quad (2)$$

with no-slip boundary conditions

$$\psi = \psi_\theta = 0 \quad \text{on} \quad \theta = 0, \alpha. \quad (3)$$

Here similarity solutions of the form $\psi = r^\lambda f(\theta)$ may be found in which the parameter λ must be determined from the eigenvalue problem resulting from (2), (3). This is evidently a similarity solution of the second kind. The most interesting feature of the solution is that, for all acute angles α (and actually over the wider range $\alpha < 147^\circ$), all relevant eigenvalues λ_i are complex, and the corresponding flows are 'eddying' flows as $r \rightarrow 0$ (Moffatt 1964a,b). The fundamental structure is precisely as indicated in Fig. 1(b).

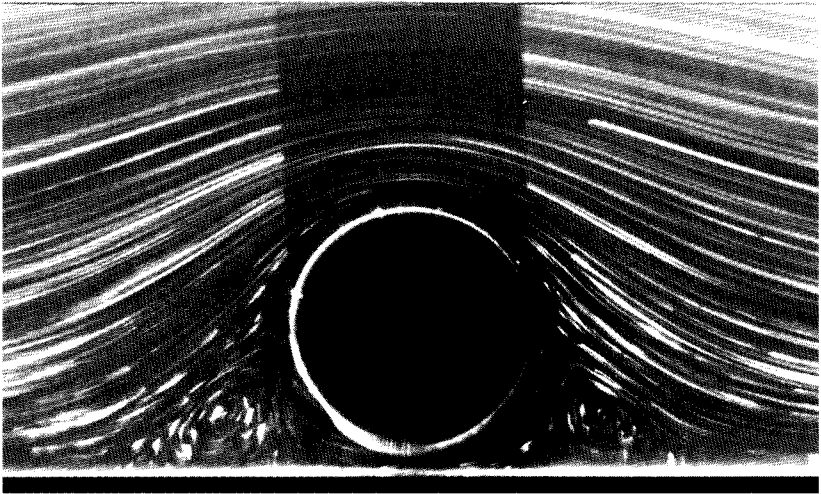


Figure 2 Corner eddies in a Stokes flow over a cylinder at a small distance from a plane boundary (Taneda 1979).

Although this was all well understood in 1964, it was not until 1979 that the first photographs of such corner eddies were published (Taneda 1979). Taneda's beautiful photographs, many of which are reproduced in Van Dyke's *Album of Fluid Motion* (1982), show a great variety of situations in which corner eddies can arise. For example, shear flow over a cylinder resting on a plane boundary shows the eddy sequence in the

two cusp-shaped regions. If the cylinder is separated from the plane by a very small amount, then a finite number of these eddies survive as attached ‘wall-eddies’ on both the plane and the cylinder (Fig. 2). If the cylinder is rotated slowly, then these eddies still survive, and may in some circumstances move into the interior of the flow (Jeffrey and Sherwood 1980). For all such situations, it is evident that an understanding of the basic prototype problem of Fig. 1(b) is the prerequisite for an analysis, whether analytical or numerical, of the more complicated configurations.

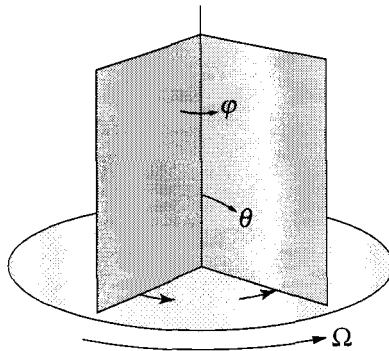


Figure 3 A three-dimensional configuration for which the Stokes flow admits a double similarity structure (Hills and Moffatt 2000).

We have recently found an example of a steady *three-dimensional* Stokes flow for which *both* types of similarity solution play a part (Hills and Moffatt 2000). The configuration is shown in Fig. 3: two fixed planes $\varphi = \pm\beta$ are ‘honed’ by rotation of the plane boundary $\theta = \pi/2$ with constant angular velocity Ω (using spherical polar coordinates (r, θ, φ)). The fluid domain is $0 < \theta < \pi/2, |\varphi| < \beta$. In the ‘Stokes’ region near $r = 0$, on dimensional grounds, the velocity field has the form

$$\mathbf{u}(r, \theta, \varphi) = \Omega r \hat{\mathbf{U}}(\theta, \varphi), \tag{4}$$

where $\hat{\mathbf{U}}(\theta, \varphi)$ is dimensionless, a similarity structure of the first kind. I use here the word ‘structure’ rather than ‘solution’, because the function $\hat{\mathbf{U}}(\theta, \varphi)$ is as yet unknown. A solution can be sought in the form $\mathbf{u} = \nabla \times (\mathbf{x}T(r, \theta, \varphi))$ where, consistent with (4), $T(r, \theta, \varphi) = \Omega r \hat{T}(\theta, \varphi)$. It turns out that, near $\theta = 0$, the solution has the form

$$\hat{T}(\theta, \varphi) = \theta^\lambda f(\varphi) \tag{5}$$

where λ is determined by precisely the same eigenvalue problem as in the two-dimensional case described previously. The flow again exhibits corner eddies (when $2\beta < 147^\circ$), which now scale with radius r (as well

as with angle θ according to (5)). We thus see a similarity solution of the second kind (5) imbedded within one of the first kind (4).

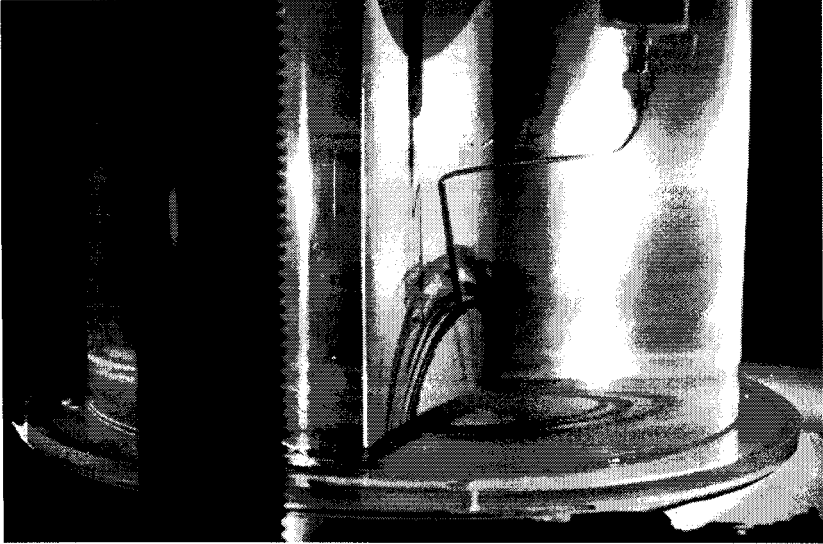


Figure 4 Closed streamlines (revealed by injection of dye) in the flow generated by rotating a horizontal plate under a fixed vertical plate (Hills and Moffatt 2000).

An experimental realization of the situation with $2\beta = \pi$ is shown in Fig. 4. The streamlines are closed, being the intersections of ‘Taylor surfaces’ $rf(\theta) = \text{const}$ and spheres $r^2 + z^2 = \text{const}$. A full analytical solution of the Stokes problem has been found for this case.

3. FREE SURFACE CUSPS

The corner flows considered above are non-analytic (or ‘singular’) in any neighborhood of the corner as a result of the imposed geometrical singularity on the boundary. I now wish to briefly consider a different type of singular behavior that occurs at a free surface and that is intrinsic to the properties of the fluid. This is the phenomenon of ‘cusping’ that occurs when flow is induced to converge towards a line on a free surface (Joseph et al. 1991, Jeong and Moffatt 1992). The prototype configuration is shown in Fig. 5: a flow driven by some stirring mechanism in the interior of the fluid of characteristic scale L say, is supposed to converge symmetrically and the surface typically dips downwards forming a cusp as indicated. An example in which the flow is driven by two counter-rotating cylinders immersed in syrup is shown in Fig. 6, in

which incidentally corner eddies can also be observed in the corners of the containing vessel.

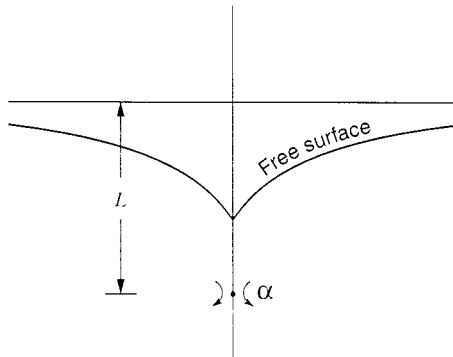


Figure 5 Prototype configuration for the formation of a free surface cusp; here, the flow is generated by a vortex dipole of strength α placed at depth L below the undisturbed free-surface level (Jeong and Moffatt 1992).

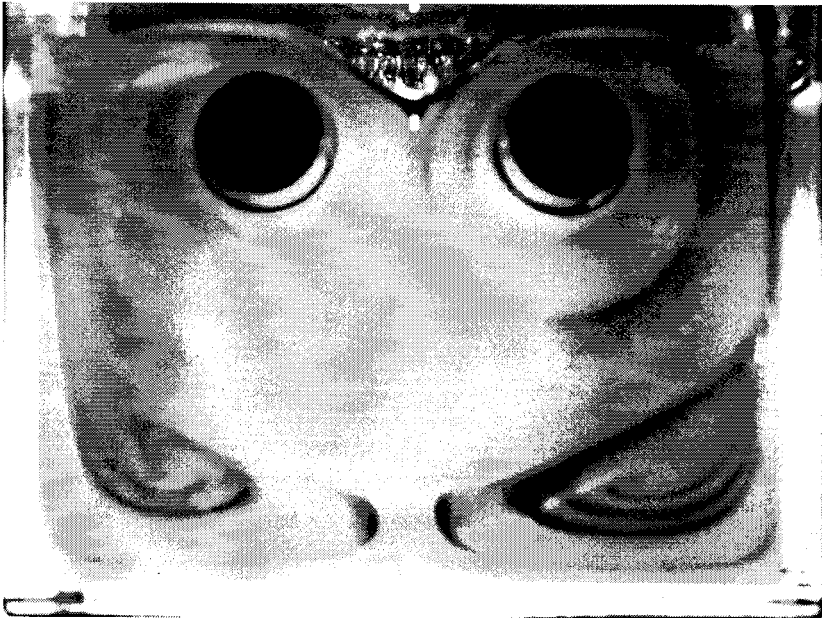


Figure 6 Free-surface cusp formed in golden syrup by the counter-rotation of two immersed cylinders (the left cylinder rotating clockwise, the right anti-clockwise). The Reynolds number is small. Note the viscous eddies in the bottom corners of the tank. [Photo courtesy of Y. Kimura]

Of course, one would expect surface tension γ to ‘round off’ the apparent cusp singularity. The small radius of curvature R at the cusp may be estimated by a purely local argument (first noted by E. J. Hinch) as follows: the surface tension provides a virtual ‘line force’ 2γ located at the center of curvature, which we take at $r = 0$ (Fig. 7). This drives a Stokeslet flow with upward velocity on the plane of symmetry

$$u = \frac{\gamma}{2\pi\mu} \ln\left(\frac{cL}{r}\right) \quad \text{for } r = O(R),$$

where c is a constant of order unity. There is also a local downward velocity U say, associated with the imposed stirring. These must equilibrate at the stagnation point on the free surface at $r = R$, i.e.

$$U = \frac{\gamma}{2\pi\mu} \ln\left(\frac{cL}{R}\right), \quad (6)$$

or equivalently,

$$\frac{R}{L} = c \exp\left(-\frac{2\pi\mu U}{\gamma}\right).$$

Thus the radius of curvature decreases exponentially with local capillary number $(\mu U/\gamma)$.

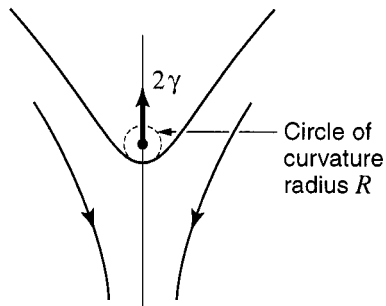


Figure 7 Representation of the flow near the free-surface stagnation point as a superposition of a two-dimensional Stokeslet and a locally uniform stream induced by remote forcing.

The details have been worked out for the idealized Stokes flow in which the stirring is induced by a vortex dipole of strength α at depth L below the (undisturbed) free surface (Jeong and Moffatt 1992). In this case, the cusp forms at depth $2L/3$ (i.e. at height $L/3$ above the vortex dipole), and the exact solution yields $U = 16\alpha/L^2$ and $c = 256/3$. Hence (6) becomes

$$\frac{R}{L} = \frac{256}{3} \exp(-32\pi C), \quad (7)$$

where $C = \mu\alpha/L^2\gamma$, the capillary number based on the 'given' flow parameters α and L . This number represents a ratio of downward viscous drag to restoring surface tension. If $C = 1$, we might anticipate that R/L should be of order unity, and so in a mathematical sense it is; however, numerically, (7) then gives

$$\frac{R}{L} \sim 10^{-42},$$

which must surely be the smallest $O(1)$ number ever encountered in a fluid dynamical context! In reality therefore a cusp *does* form, and there is an associated stress singularity that is presumably resolved only if non-Newtonian and/or non-continuum effects are taken into account.

In a region $R \ll r \ll L$, the streamfunction of the 'cusp' flow within the fluid is given in polar coordinates (r, θ) by

$$\psi \sim 16\alpha r \cos \theta - \frac{8\sqrt{6}\alpha r^{3/2}}{L^{1/2}} \sin^3\left(\frac{1}{2}\theta\right).$$

The second term shows a self-similar structure, the same as that associated with a symmetric flow near the edge of a flat plate $\theta = \pm\pi$.

Although the cusping phenomenon has been analyzed only within the Stokes approximation, I believe that it occurs quite generally in high Reynolds number flow also, and that many observed phenomena can be explained only through an understanding of the cusping mechanism. I show one example in Fig. 8, which shows a spherical cap bubble rising in glycerine in the bubble tube at DAMTP, Cambridge. This bubble is in the 'wavy-skirted regime' characterized by the very thin film of air entrained into the glycerine from the sharp edge of the bubble. The flow is converging near this sharp edge, and it is therefore presumably cusped. The skirt forms because of the large air pressure generated in this cusp region.

Similarly, when water runs smoothly into a deep bath (the 'Japanese bath problem'), it may be observed that, above a critical flow rate, bubbles of air are entrained and the pouring suddenly becomes noisy as a result of bubble oscillation. I believe that this entrainment of bubbles must occur through the circular cusp that forms where the incoming jet of water impinges on the free surface (Fig. 9).

4. GLOBAL INVARIANTS

Let me pass now to the opposite situation, namely the unsteady fully three-dimensional flow of a strictly inviscid, incompressible fluid (of course an idealization). This is the classical fluid dynamics of Helmholtz



Figure 8 The rise of a wavy skirted bubble through the common room of DAMTP, Cambridge. The bubble tube, of diameter 17 cm contains glycerine. The portrait is of A. S. Eddington.

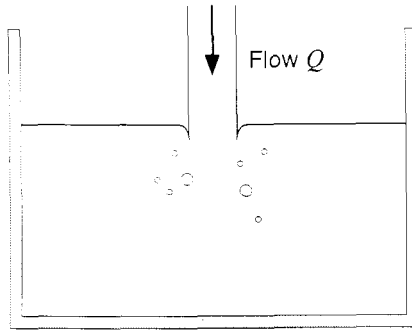


Figure 9 The Japanese bath problem: a laminar stream of water flows into a deep bath; above a critical flow rate Q_c , bubbles are entrained through the circular cusp formed at the free surface.

and Kelvin, for which we know that the circulation round every material (i.e. Lagrangian) circuit is conserved. A closely related result (J.-J.

Moreau 1961, Moffatt 1969) is that the helicity

$$\mathcal{H} = \int_V \mathbf{u} \cdot \boldsymbol{\omega} \, dV$$

for any material volume V , on whose surface $\boldsymbol{\omega} \cdot \mathbf{n} = 0$, is also conserved; here, $\boldsymbol{\omega} = \text{curl } \mathbf{u}$ is the vorticity field. This conservation of helicity admits topological interpretation: it is, in a sense that can be refined (Arnol'd 1974), the degree of linkage of constituent vortex tubes in the flow, a linkage that, as recognized by Kelvin, is indeed conserved.

An analogous result holds in the magnetohydrodynamics (MHD) of perfectly conducting fluids, in which lines of magnetic field \mathbf{B} (or ' \mathbf{B} -lines') are frozen in the fluid. The analogous conserved quantity is the magnetic helicity

$$\mathcal{H}_M = \int_V \mathbf{A} \cdot \mathbf{B} \, dV$$

where $\mathbf{B} = \text{curl } \mathbf{A}$, and it admits similar topological interpretation. It is in this MHD context that the concept of helicity has proved to have profound significance, in two quite complementary situations:

4.1. The turbulent dynamo

I believe that the most important fundamental breakthrough of the last half-century in our understanding of turbulent processes relates to the dynamo problem: under what circumstances will a magnetic field $\mathbf{B}(\mathbf{x}, t)$ systematically increase in intensity under the distorting and diffusive action of a field of stationary homogeneous turbulence $\mathbf{u}(\mathbf{x}, t)$? The question was posed first in this form by Batchelor (1950). The simple answer is that a sufficient condition for such dynamo action is that the turbulence should 'lack reflectional symmetry'; the simplest measure of such lack of reflectional symmetry is the mean helicity of the turbulence $\langle \mathbf{u} \cdot \boldsymbol{\omega} \rangle$, and if this mean helicity is non-zero, then dynamo action will in general occur (Steenbeck, Krause, and Rädler 1966, Moffatt 1970). This result has huge implications for current understanding of the process by which magnetic fields are generated in planets, stars and galaxies; it is in more senses than one, a truly global phenomenon.

4.2. Relaxation to equilibrium states

The relaxation process is the converse of the dynamo process and is best illustrated by simple example. Suppose that at some initial instant $t = 0$, a magnetic field $\mathbf{B}_0(\mathbf{x})$ having some nontrivial knotted or linked structure is imbedded in a perfectly conducting, but viscous, incompressible fluid at rest. The prototype consisting of two linked, unknotted

ted flux tubes, is shown in Fig. 10. The current corresponding to \mathbf{B}_0 is $\mathbf{j}_0 = \text{curl } \mathbf{B}_0$, the Lorentz force distribution $\mathbf{F}_0 = \mathbf{j}_0 \times \mathbf{B}_0$ is in general rotational, and the fluid must flow in response to this force. Thus magnetic energy is converted to kinetic energy as in an electric motor, and this is dissipated by viscosity. However, the topology of the field $\mathbf{B}(\mathbf{x}, t)$ is conserved, since the lines of force are frozen in the fluid and deform continuously with the flow. In particular, the magnetic helicity, which in this special case is $\mathcal{H}_M = 2\Phi_1\Phi_2$ where Φ_1 and Φ_2 are the fluxes in the two tubes, is conserved.

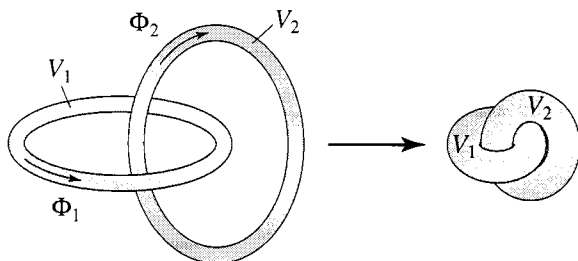


Figure 10 Prototype configuration for the problem of magnetic relaxation: two linked flux tubes contract in a perfectly conducting fluid, with fluxes and volumes conserved, until the linkage prevents further contraction (Moffatt 1985).

We are thus faced with the problem (Arnol'd 1974, Moffatt 1985) of minimizing magnetic energy subject to conservation of field topology; more precisely, of finding minimum energy states that are topologically accessible from the initial state. In these states, the Lorentz force is irrotational, since the fluid must come to rest, i.e.

$$\mathbf{j} \times \mathbf{B} = \nabla p, \quad \mathbf{j} = \text{curl } \mathbf{B}, \quad (8)$$

for some scalar field p (evidently the pressure field). This process of magnetic relaxation is brought about in physical terms through relaxation of the Maxwell stress in each flux tube, as illustrated in Fig. 10. The tubes contract in axial length, and since volume is conserved, their cross sections increase in area. The topological constraint arrests the relaxation process when the tubes ultimately make contact: a singularity (here a surface discontinuity) inevitably appears as $t \rightarrow \infty$ (it may occur at finite time, but this seems unlikely).

Equation (8) has precisely the same structure as the Euler equation for steady flow of an inviscid incompressible fluid:

$$\mathbf{u} \times \boldsymbol{\omega} = \nabla h, \quad \boldsymbol{\omega} = \text{curl } \mathbf{u}, \quad (9)$$

where $h = p/\rho + \frac{1}{2}\mathbf{u}^2$ and ρ is the fluid density (assumed constant). To every solution of (8), there corresponds a solution of (9) via the analogy

$$\mathbf{B} \rightarrow \mathbf{u}, \quad \mathbf{j} \rightarrow \boldsymbol{\omega}, \quad p \rightarrow h_0 - h,$$

where h_0 is an arbitrary constant. Thus, magnetic relaxation provides an indirect means of proving the existence of steady Euler flows (solutions of (9)) of arbitrarily complex streamline topology; consideration of their stability is quite another matter (Moffatt 1986; see also Vladimirov, Moffatt, and Ilin 1999).

5. **EXISTENCE OF SMOOTH SOLUTIONS OF THE NAVIER–STOKES EQUATIONS FOR ALL $T > 0$**

The problem of existence and smoothness for the Navier–Stokes (NS) equations was addressed by Leray (1934) and has attracted intense effort in the mathematical community since then. Despite these efforts, the problem remains open; it has recently achieved millennial status as one of the seven problems identified by the Clay Institute for which a prize of one million dollars is offered. Charles Fefferman has given details for the NS problem on the website of the Clay Institute.

I don't propose to solve this problem today! I do wish however to make some observations about it, because it seems to me that both local and global considerations are likely to play a part in its solution.

Leray himself was unable to prove the existence of smooth solutions of the NS equations in 3 dimensions for all $t > 0$, and recognized the alternative possibility that a singularity may develop at finite time, t^* say. If such a singularity develops at a point that we may take to be $\mathbf{x} = \mathbf{0}$, then it seems plausible that the approach to this singularity (as $t \rightarrow t^*$) should be at least locally self-similar. Leray noted a remarkable similarity transformation of the NS equations, or equivalently of the vorticity equation

$$\frac{\partial \boldsymbol{\omega}}{\partial t} = \nabla \times (\mathbf{u} \times \boldsymbol{\omega}) + \nu \nabla^2 \boldsymbol{\omega}. \tag{10}$$

This transformation is

$$\mathbf{X} = \frac{\mathbf{x}}{(\Gamma(t^* - t))^{1/2}}, \quad \mathbf{u}(\mathbf{x}, t) = \frac{\Gamma^{1/2}}{(t^* - t)^{1/2}} \mathbf{U}(\mathbf{X}),$$

where Γ is a constant with the dimensions of circulation (velocity \times length). The vorticity then transforms as

$$\boldsymbol{\omega} = \text{curl } \mathbf{u} = \frac{1}{t^* - t} \boldsymbol{\Omega}(\mathbf{X}), \quad \boldsymbol{\Omega} = \text{curl}_{\mathbf{x}} \mathbf{U}, \tag{11}$$

and equation (10) transforms to

$$0 = \nabla \times (\mathbf{U} + \frac{1}{2}\mathbf{X}) \times \boldsymbol{\Omega} + \epsilon \nabla^2 \boldsymbol{\Omega}, \quad (12)$$

where $\epsilon = \nu/\Gamma$, a dimensionless parameter that we may assume to be small. The (\mathbf{x}, t) problem of (10) is thus converted to a ‘steady’ problem (12) in the scaled space variable \mathbf{X} . The term $\partial\boldsymbol{\omega}/\partial t$ in (10) transforms to the term $\frac{1}{2}\nabla \times (\mathbf{X} \times \boldsymbol{\Omega})$ in (12), which represents outward transport of the vorticity field $\boldsymbol{\Omega}$ by the steady spherically symmetric ‘compressible velocity field’ $\frac{1}{2}\mathbf{X}$. The question now is whether there exists a distribution of vorticity such that the corresponding velocity \mathbf{U} in conjunction with diffusion can compensate this outward transport.

For reasons developed in a recent paper (Moffatt 2000a), it is relevant to seek solutions of (12) in an inner region (in the sense of matched asymptotic expansions) for which $\boldsymbol{\Omega}(\mathbf{X})$ matches with $\boldsymbol{\omega}(\mathbf{x}, t)$ (the outer solution) in an overlap region $\mathbf{X} \rightarrow \infty$, $\mathbf{x} \rightarrow \mathbf{0}$. At leading order, this seems to require that

$$\mathbf{U}(\mathbf{X}) \sim \frac{1}{|\mathbf{X}|}, \quad \boldsymbol{\Omega}(\mathbf{X}) \sim \frac{1}{|\mathbf{X}|^2} \text{ as } \mathbf{X} \rightarrow \infty, \quad (13)$$

with corresponding outer behavior

$$|\mathbf{u}| \sim \frac{\Gamma}{|\mathbf{x}|}, \quad \boldsymbol{\omega} \sim \frac{\Gamma}{|\mathbf{x}|^2} \text{ as } |\mathbf{x}| \rightarrow 0.$$

(This, incidentally, is suggestive of Stokeslet behavior, which might be thought to require a source of momentum in the inner region, and thus to be incompatible with unforced evolution!)

It has been shown by Nečas, Růžička and Šverák (1996) that no smooth nontrivial solution of (12) exists (with $\epsilon > 0$) for which $|\mathbf{U}| \in L^3(\mathbb{R}^3)$. The behavior (13) is just at the boundary of this function space, and is not excluded by the theorem.

A vorticity singularity as represented by (11) can occur only through stretching of vortex lines at a rate that also becomes infinite as $t \rightarrow t^*$. Such a process can conceivably occur through the nonlinear interaction of vortex tubes each one of which provides the strain field acting on the other. Some mechanism must be present to cause all length scales in the inner region to decrease to zero (like $(t^* - t)^{1/2}$) as $t \rightarrow t^*$. Scenarios involving the collision of non-parallel vortex pairs seem plausible candidates (Pelz 1997, Moffatt 2000a), the collision zone being then the inner region in which the Leray transformation is relevant. An alternative scenario is sketched in Fig. 11, which shows a vortex pair knotted in the internal zone and arranged in the external zone in such a way as to

‘pull the knot tight’. This is certainly suggestive of how a finite-time singularity may arise if the initial conditions are sufficiently ingeniously contrived.

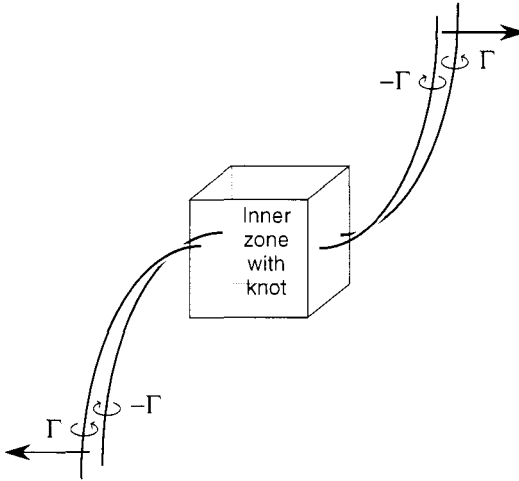


Figure 11 Conceptual sketch of a vortex pair configuration for which propagation of the pair in the external region leads to tightening of any knot that may be contained within the inner region (here represented simply by a ‘black box’).

Topology evidently plays a part in this. Note that the contribution to helicity from any region $V(t)$: $|\mathbf{X}| < R$ (with R constant) of the inner zone is given by

$$\mathcal{H} = \int_V \mathbf{u} \cdot \boldsymbol{\omega} \, d^3\mathbf{x} = \Gamma^2 \int_0^R \mathbf{U} \cdot \boldsymbol{\Omega} \, d^3\mathbf{X},$$

and that this is independent of time. This suggests conservation of topology of vortex tubes in the inner region *despite the influence of viscosity*. It is perhaps here that one may find a clue for the relevance of global (i.e. topological) considerations for the NS singularity problem.

6. A TOY MODEL OF A FINITE-TIME SINGULARITY

It may be appropriate to conclude this lecture with a real finite-time singularity! This is exhibited by the toy ‘Euler’s disk’, a heavy disk that rolls on its edge (Fig. 12), and exhibits a paradoxical increase of rolling speed as its energy decreases (Bendik 2000). The energy E is equal to $\frac{3}{2}Mga\alpha$ ($M = \text{mass}$, $a = \text{radius}$) when the angle α between the disk and the table is small (i.e. during the final ‘shuddering’ phase of motion).

The rolling (precessional) speed Ω is related to α during this phase by the equation

$$\Omega^2 \alpha = \frac{4g}{a}, \quad (14)$$

a consequence of Euler's angular momentum equation, coupled with the rolling condition. As α tends to zero, then for so long as (14) holds (the 'adiabatic approximation'), Ω increases like $\alpha^{-1/2}$, apparently without limit. The interesting feature of this toy is that the phenomenon can indeed be observed at finite time (of the order of 10^2 s) after the disk is set in motion; I demonstrate this here with the aid of a microphone to amplify the increasing frequency Ω and the very abrupt stop. Reflection of a laser from the surface of the disk onto a screen can be used to visualize and measure the decrease of α as a function of time.

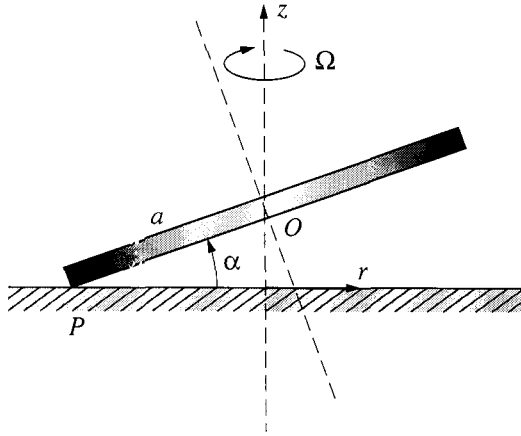


Figure 12 Euler's disk: a heavy circular disk rolls on its rim with precessional angular velocity Ω . The system exhibits a finite-time singularity induced by weak dissipative processes (Moffatt 2000b).

The energy equation is

$$\frac{dE}{dt} = -\Phi(E), \quad (15)$$

where Φ is the rate of dissipation of energy, whatever the dominant dissipative mechanism may be. If $\Phi(E) \propto E^\lambda$ where $\lambda < 1$, (15) implies that E goes to zero at finite time, t^* say, and hence that, within the adiabatic approximation, $\Omega \rightarrow \infty$ as $t \rightarrow t^*$. If $\lambda < 0$, then obviously $dE/dt \rightarrow \infty$ also as $t \rightarrow t^*$, and the settling process may reasonably be described as 'dramatic'. The behavior is familiar to anyone who has spun a coin upon a table. (It is to be contrasted with, for example,

linear damping of a simple pendulum, for which $\lambda = 1$, and the decay is exponential.)

The viscosity of the air in the thin layer between the disk and the table in the final shuddering phase provides one obvious dissipative mechanism for which $\Phi(E)$ may be calculated (Moffatt 2000b). A lubrication approximation gives $\lambda = -2$; an improved analysis allowing for Stokes layers on the disk and table (L. Bildsten, private communication) gives $\lambda = -5/4$. Either way, the finite-time singularity is dramatic.

There is also a contribution to dissipation from rolling friction, which is apparently much more difficult to quantify. On the simple assumption that for this mechanism $\Phi \propto \Omega$, (14) with $E \propto \alpha$ gives $\lambda = -\frac{1}{2}$, and again the behavior is dramatic. The difficulty here is to obtain the coefficient of proportionality between Φ and Ω in terms of the physical properties of the disk and the table—a challenging problem that perhaps someone in this large audience knows how to solve.

It is likely that different dissipative mechanisms dominate at different stages of the settling process, and that the effect of air viscosity is dominant only in the very final stage before the sudden stop. The predicted singularity is resolved during the final few microseconds, when the downward vertical acceleration of the center-of-mass of the disk becomes comparable with the acceleration of gravity (Moffatt 2000b).

7. CONCLUSION

The smoothness, or alternatively the finite-time singularity, of the Navier–Stokes equations offers a challenge that will continue to make great demands on both analytical ingenuity and computational power. If, as computer simulations continue to indicate (Kerr 1997), a finite-time singularity does occur and if this is generic behavior, then of course we shall have to understand by what mechanism these putative singularities are resolved. Since the pressure gradient must also become unbounded as a singularity is approached, the incompressibility assumption, on which most analyses of this phenomenon are based, becomes no longer tenable. The infinite stress at a singularity can be relieved by cavitation in liquids, and by acoustic radiation in gases. The Japanese bath provides a congenial environment for the contemplation of such problems!

As I mentioned in my introductory remarks, this Congress exhibits a most fruitful interplay between local and global characteristics. I would maintain now that it also has some features of a finite-time singularity: there was certainly a decreasing length-scale as we all converged on Chicago; and the Organizers were acutely aware of a decreasing time-scale in the last few weeks of hectic preparations. We should be relieved

that the Marriott Hotel has neither imploded nor exploded under the extreme pressure of activity that it has experienced this week. Now we are at the stage where the singularity must be resolved; we shall return to our homes around the world like acoustic pulses radiating from this source, and the locally acquired impact of this Congress will surely inform and inspire future research in theoretical and applied mechanics on a global scale. On that note, and like a finite-time singularity, I must bring this talk to a sudden end.

Acknowledgments

I thank Sarah Kirkup and Jonathan Chin for help in processing the text and figures; and Mustapha Amrani for help in preparing the powerpoint version of the lecture.

References

- Arnol'd, V. I. 1974. The asymptotic Hopf invariant and its applications. [English translation: *Selecta Mathematica Sovietica* **5**, 327–345 (1986)]
- Barenblatt, G. I. 1979. *Similarity, Self-similarity and Intermediate Asymptotics*. New York: Plenum.
- Batchelor, G. K. 1950. On the spontaneous magnetic field in a conducting liquid in turbulent motion. *Proceedings of the Royal Society A* **201**, 405–416.
- Bendik, J. 2000. Website: <http://www.eulerdisk.com>
- Burgers, J. M. 1948. A mathematical model illustrating the theory of turbulence. *Advances in Applied Mechanics* **1**, 171–199.
- Hancock, C., H. K. Moffatt, and E. Lewis. 1981. Effects of inertia in forced corner flows. *Journal of Fluid Mechanics* **112**, 315–327.
- Hills, C. P., and H. K. Moffatt. 2000. Rotary honing: a variant of the Taylor paint-scraper problem. *Journal of Fluid Mechanics* **418**, 119–135.
- Jeffrey, D. J., and J. D. Sherwood. 1980. Streamline patterns and eddies in low-Reynolds-number flow. *Journal of Fluid Mechanics* **96**, 315–334.
- Jeong, J.-T., and H. K. Moffatt. 1992. Free-surface cusps associated with flow at low Reynolds number. *Journal of Fluid Mechanics* **241**, 1–22.
- Joseph, D. D., J. Nelson, M. Renardy, and Y. Renardy. 1991. Two-dimensional cusped interfaces. *Journal of Fluid Mechanics* **223**, 383–409.
- Kerr, R. M. 1997. Euler singularities and turbulence. In *Proceedings of the 19th International Congress of Theoretical and Applied Mechanics* (T. Tatsumi, E. Watanabe, and T. Kambe, eds.). Amsterdam: Elsevier Science Publishers, 57–70.
- Leray, J. 1934. Sur le mouvement d'un liquide visqueux emplissant l'espace. *Acta Mathematica* **63**, 193–248.
- Moffatt, H. K. 1964a. Viscous and resistive eddies near a sharp corner. *Journal of Fluid Mechanics* **18**, 1–18.
- Moffatt, H. K. 1964b. Viscous eddies near a sharp corner. *Archiwum Mechaniki Stosowanej* **2**, 365–372.
- Moffatt, H. K. 1969. The degree of knottedness of tangled vortex lines. *Journal of Fluid Mechanics* **36**, 117–129.

- Moffatt, H. K. 1970. Turbulent dynamo action at low magnetic Reynolds number. *Journal of Fluid Mechanics* **41**, 435–452.
- Moffatt, H. K. 1985. Magnetostatic equilibria and analogous Euler flows of arbitrarily complex topology, Part 1, Fundamentals. *Journal of Fluid Mechanics* **159**, 359–378.
- Moffatt, H. K. 1986. Magnetostatic equilibria and analogous Euler flows of arbitrarily complex topology, Part 2, Stability considerations. *Journal of Fluid Mechanics* **166**, 359–378.
- Moffatt, H. K. 2000a. The interaction of skewed vortex pairs: a model for blow-up of the Navier–Stokes equations. *Journal of Fluid Mechanics* **409**, 51–68.
- Moffatt, H. K. 2000b. Euler’s disk and its finite-time singularity. *Nature* **404**, 833–834.
- Moreau, J.-J. 1961. Constantes d’un îlot tourbillonnaire en fluide parfait barotrope. *Comptes Rendus à l’Académie des Sciences, Paris* **252**, 2810–2813.
- Nečas, J., M. Růžička, and V. Šerák. 1996. On Leray’s self-similar solutions of the Navier–Stokes equations. *Acta Mathematica* **176**, 283–294.
- Pelz, R. B. 1997. Locally self-similar finite-time collapse in a high-symmetry vortex filament model. *Physical Review E* **55**, 1617–1626.
- Steenbeck, M., F. Krause, and K.-H. Rädler. 1966. Berechnung der mittleren Lorentz-Feldstärke $\overline{\mathbf{v} \times \mathbf{B}}$ für ein elektrisch leitendes Medium in turbulenter, durch Coriolis-Kräfte beeinflusster Bewegung. *Zeitschrift Naturforschung Teil A* **21**, 369–376.
- Taneda, S. 1979. Visualization of separating Stokes flows. *Journal of the Physical Society of Japan* **46**, 1935–1942.
- Taylor, G. I. 1960. Similarity solutions of hydrodynamic problems. In *Aeronautics and Astronautics* (Durand Anniversary Volume). New York: Pergamon, 21–28.
- Van Dyke, M. 1982. *An Album of Fluid Motion*. Stanford, Calif.: Parabolic Press.
- Vladimirov, V. A., H. K. Moffatt, and K. I. Il’in. 1999. On general transformations and variational principles for the magnetohydrodynamics of ideal fluids. Part 4. Generalized isovorticity principle for three-dimensional flows. *Journal of Fluid Mechanics* **390**, 127–150.